

Dietary cholesterol withdrawal reduces vascular inflammation and induces coronary plaque stabilization in miniature pigs

Peter Verhamme^a, Rozenn Quarck^a, Hiroyuki Hao^b, Michiel Knaapen^c,
Steven Dymarkowski^d, Hilde Bernar^a, Johan Van Cleemput^e, Stefan Janssens^e,
Jozef Vermeylen^f, Giulio Gabbiani^b, Mark Kockx^c, Paul Holvoet^{a,*}

^aCardiovascular Research Unit, Center for Experimental Surgery and Anesthesiology, KU Leuven, Campus Gasthuisberg, O&N, Herestraat 49, B-3000 Leuven, Belgium

^bDepartment of Pathology, University of Geneva–CMU, Geneva, Switzerland

^cAZ-Middelheim and Department of Pharmacology, University of Antwerp, Antwerp, Belgium

^dDepartment of Radiology, UZ Leuven, Leuven, Belgium

^eDepartment of Cardiology, UZ Leuven, Leuven, Belgium

^fCenter for Molecular and Vascular Biology, KU Leuven, Belgium

Received 18 April 2002; accepted 6 June 2002

Abstract

Objective: To study the effect of dietary cholesterol withdrawal on size and composition of LDL-hypercholesterolemia-induced coronary plaques in miniature pigs. **Methods:** Pigs were on normal chow (control group), on a cholesterol-rich diet for 37 weeks (hypercholesterolemic group) or on a cholesterol-rich diet followed by normal chow for 26 weeks (cholesterol withdrawal group). Endothelial function was assessed with quantitative angiography after intracoronary infusion of acetylcholine, plaque load with intra-coronary ultrasound and plaque composition with image analysis of cross-sections. The effect of porcine serum on coronary smooth muscle cell (SMC) function was studied in vitro. **Results:** Cholesterol-rich diet caused LDL-hypercholesterolemia, increased plasma levels of oxidized LDL (ox-LDL) and C-reactive protein (CRP), and induced endothelial dysfunction and coronary atherosclerosis. Dietary cholesterol withdrawal lowered LDL, ox-LDL and CRP. It restored endothelial function, did not affect plaque size but decreased lipid, ox-LDL and macrophage content. Smooth muscle cells and collagen accumulated within the plaque. Increased smoothelin-to- α -smooth muscle actin ratio indicated a more differentiated SMC phenotype. Cholesterol lowering reduced proliferation and apoptosis. In vitro, hypercholesterolemic serum increased SMC apoptosis and decreased SMC migration compared to non-hypercholesterolemic serum. **Conclusions:** Cholesterol lowering induced coronary plaque stabilization as evidenced by a decrease in lipids, ox-LDL, macrophages, apoptosis and cell proliferation, and an increase in differentiated SMC and collagen. Increased migration and decreased apoptosis of SMC may contribute to the disappearance of the a-cellular core after lipid lowering.

© 2002 Elsevier Science B.V. All rights reserved.

Keywords: Atherosclerosis; Cholesterol; Endothelial function; Lipoproteins; Smooth muscle

1. Introduction

Lipid lowering reduces cardiovascular morbidity and mortality in a broad range of patients [1]. Lipid lowering trials showed only minimal increase in coronary artery lumen [2]. However, the risk for coronary events in these trials was reduced by up to 70%, suggesting that the

benefit of lipid lowering goes far beyond plaque regression [2]. Acute coronary syndromes most frequently involve thrombosis triggered by the rupture of an atherosclerotic plaque that typically consists of a large lipid core with a thin fibrous cap and shoulder regions that are heavily infiltrated by inflammatory cells [3]. The clinical benefit of lipid lowering may greatly depend on reduced vascular inflammation and plaque stabilization [4].

*Corresponding author. Tel.: +32-16-347-149; fax: +32-16-347-114.
E-mail address: paul.holvoet@med.kuleuven.ac.be (P. Holvoet).

Time for primary review 26 days.

We have previously reported that miniature pigs develop LDL-hypercholesterolemia and advanced coronary atherosclerosis within 6–9 months when fed a cholesterol-rich diet [5]. The aim of this study was to investigate the effects of dietary cholesterol withdrawal on coronary endothelial function, plaque size and composition of advanced coronary plaques. We determined the relative macrophage, smooth muscle cell (SMC) and collagen content of coronary plaques and the number of apoptotic and proliferating cells. The degree of SMC differentiation was studied by determining the number of smoothelin positive SMC. Smoothelin is a marker of the differentiated SMC phenotype [6].

Previous studies have investigated the effect of dietary lipid lowering in animal models of diet-induced atherosclerosis. Atherosclerosis was induced in the thoracic aorta of rabbits by a cholesterol-rich diet [7] or by combining cholesterol-rich diet with injury [8,9]. Dietary lipid lowering reduced macrophage infiltration, lipid content and apoptosis and promoted accumulation of collagen and SMC in the thoracic aorta of rabbits [7–9]. Both the lipid profile and the composition of thoracic atherosclerotic lesions in rabbits differ however from the human lipid profile and the composition of human coronary plaques. The lipid profile, more particularly the occurrence of LDL hypercholesterolemia, and the composition of advanced coronary plaques in hypercholesterolemic miniature pigs better reflect hypercholesterolemia and coronary atherosclerosis in man. The effect of dietary cholesterol lowering was also investigated in the thoracic aorta [10] and coronary arteries in primates [11,12]. Lipid depletion of the coronary arteries was demonstrated 6 months after dietary lipid lowering, whereas regression of the atherosclerotic lesion was observed 20 months after dietary lipid lowering [13]. The mechanisms underlying the repopulation of the a-cellular core with smooth muscle cells was however not investigated in those studies. The aims of this study were therefore to study the effect of cholesterol withdrawal on stabilization of advanced coronary plaques and more particularly to investigate the repair mechanisms that lead to the repopulation of the a-cellular core with smooth muscle cells after cholesterol lowering. We therefore investigated in vitro the effect of normal and hypercholesterolemic serum on the migration, proliferation, apoptosis and matrix production by coronary artery-derived smooth muscle cells.

2. Methods

2.1. Animal procedures

The investigation conforms the *Guide for the Care and Use of Laboratory Animals* published by the US National Institutes of Health (NIH Publication No. 85-23, revised 1996). The Institutional Review Board of the KU Leuven

approved all animal procedures. Miniature pigs were obtained by crossbreeding Göttinger and Yucatan miniature pigs (Charles River Laboratories) as described earlier [5]. A total of 14 pigs were on normal chow (control group), while 12 age-matched pigs were on an atherogenic diet containing 4% cholesterol, 14% beef tallow and 2% hog bile at a daily amount of 1 kg/day starting at the age of 4 months for 37 ± 5 (mean \pm S.D.) weeks (hypercholesterolemic group). A total of seven pigs were on the atherogenic diet for 40 ± 1 weeks followed by normal chow for 26 ± 1 weeks (cholesterol withdrawal group).

2.2. Blood sampling and analysis

Peripheral venous blood was drawn from an ear vein. Total cholesterol, HDL cholesterol and triglyceride levels were measured by enzymatic methods (Boehringer Mannheim, France). LDL cholesterol levels were calculated with the Friedewald formula. Plasma ox-LDL was measured as described before [14]. In vitro porcine ox-LDL was prepared as described before [14]. Plasma levels of CRP were measured with an immunoturbidimetric assay (Roche) with a detection limit of 3 mg/l.

2.3. Anesthesia

Pigs received intramuscular (i.m.) injections of 250 mg/day aspirin for 3 days prior to procedures. Pigs were sedated with azaperone (0.1 ml/kg i.m.). Anesthesia was induced with 10 mg/kg ketamine i.m., 0.1 ml/kg xylazine and 5 mg/kg sodium pentobarbital i.v. Pigs were intubated and ventilated with O₂-enriched room air. Anesthesia was maintained with a continuous infusion of 2–5 mg/kg per h propofol after a loading dose of 100 mg, i.v. ECG and arterial pressure were continuously monitored.

2.4. Coronary artery instrumentation

The left carotid artery was exposed, an 8F arterial introducer sheath was inserted and a left Judkins guiding catheter was advanced into the aortic root. Then 15,000 IU heparin and 250 mg acetyl salicylic acid, 15 mg lidocaine and 100 mg bretylate were administered i.v. [15]. A 2.2F coronary infusion catheter (Boston Scientific) was positioned in the proximal left anterior descending coronary artery (LAD).

2.5. In vivo endothelial reactivity

Endothelial function was assessed in all pigs of the cholesterol withdrawal group before and after cholesterol withdrawal, and in nine age-matched control pigs. Baseline angiographies were recorded after 5 min of saline infusion. To assess endothelium-dependent vasoreactivity, acetylcholine (Miochol, Cibavision) was infused at a concentration of 10^{-4} M at 1 ml/min for 3 min [16]. Nitro-

glycerin (200 µg) was injected as an intracoronary bolus through the guiding catheter to assess endothelium independent vasoreactivity. Hemodynamic data and coronary angiographies were obtained at every phase. Coronary artery diameter of three end-diastolic frames 5–10 mm distal from the infusion catheter was measured using quantitative angiography software (Quantcor.QCA V2.0). The percentage change in coronary diameter after acetylcholine and after nitroglycerine versus baseline was calculated.

2.6. Intracoronary ultrasound

Intracoronary ultrasound (ICUS) of the LAD was performed to assess vessel and lesion size. In the control and hypercholesterolemic group ICUS was performed at sacrifice. In the cholesterol withdrawal group, ICUS was performed before cholesterol withdrawal and at sacrifice. A 0.014" guide wire (Cordis, Belgium) was advanced into the LAD and a 3F 64-MHz multi-array IVUS probe (IVUS Visions Five-64F/X, Endosonics, Belgium) was placed in the LAD. Automatic pullback video loops of the proximal LAD were recorded and stored on CD-ROM for off-line analysis. Total vessel, intimal and lumen areas were determined in ten frames of the LAD proximal from D1 and averaged.

2.7. Sacrifice and coronary artery sampling

The chest was opened in deep pentobarbital and ketamine anesthesia. Pigs were injected with saturated potassium chloride solution to induce ventricular fibrillation and the heart was excised.

The coronary artery system was flushed and pressure perfusion fixed at 100 mmHg with 1500 ml of 4% paraformaldehyde in PBS (PFA). The coronary arteries were excised and the LAD was divided into twelve 3-mm rings. One half was cryo-embedded in tissue freezing medium by immersion in pre-cooled 2-methylbutane and stored until sectioning at -80°C . The other half was immersed in 70% ethanol and subsequently paraffin embedded.

2.8. Morphometric analysis of coronary lesions

Sections (7 µm) of the proximal LAD were stained with hematoxylin-eosine to assess lesion size and ICUS was also performed. An average of 18 sections spanning a 3-mm segment of the LAD were measured and averaged. Morphometric analysis of sections was performed using the Leica Quantimet 600 image analysis system (Leica, Brussels, Belgium). Total lipid deposition in the lesions was determined in oil-red-O stained sections. The total amount of collagen in the lesion was determined on picrosirius red stained sections viewed in normal light. Triple helix collagen was measured on the same sections

viewed in polarized light [17]. Elastin content was measured on Verhoeffs-stained sections and by measuring autofluorescence of the coronary lesion [18,19]. Lesions in the hypercholesterolemic and the cholesterol withdrawal group were classified using the Stary classification into early lesions (Stary I–III) and more advanced lesions (Stary classification IV and above) [20].

2.9. Immunohistochemistry

On frozen sections, macrophages were stained with the swine specific mAb 74-12-25, ox-LDL with the mAbs M1H11 and OX4E6 [21], myeloperoxidase with the mAb MPO-7 (Dako), and collagen type I with mAb I-8H5 (ICN). α -SM actin and smoothelin were detected with a mouse monoclonal IgG2a recognizing α -SM actin or a mouse monoclonal IgG1 cross-reacting with smoothelin as previously described [22,23]. In advanced lesions, stained areas on ten sections were measured using the Quantimet 600 image analyzer in color detection mode as described earlier [21].

2.10. Proliferation and apoptosis

Replicating cells were detected with the Ki67-specific monoclonal antibody MIB-1 (Immunotech). Double staining for α -actin and Ki67 was performed to detect replicating SMC. A modified TUNEL protocol was used for the detection of apoptotic cells in atherosclerotic plaques [7]. Total cell density was measured and proliferating and apoptotic cells were counted. Five sections per lesion were analyzed and numbers were averaged. TUNEL staining was combined with PAS staining to identify apoptotic SMC surrounded by a PAS-positive cage [7]. Caspase-3 positive cells were stained with the polyclonal antibody H-277 (Santa-Cruz).

2.11. Smooth muscle cell culture

SMC of coronary arteries from miniature pigs were isolated using the explant-outgrowth method [24]. Cells were maintained in culture in Dulbecco's modified essential medium (DMEM) supplemented with 10% fetal bovine serum (FBS), 100 U/ml penicillin and 100 µg/ml streptomycin. All experiments were performed with cells of less than five passages.

2.11.1. SMC apoptosis

Cells were seeded on two or four chamber glasses till sub-confluent and starved for 48 h with DMEM-FBS 0.2%. Thereafter, cells were incubated with DMEM supplemented with either 0.2% FBS, 10% FBS, 10% control pig serum (CPS), 10% hypercholesterolemic pig serum (HPS), 10% pig serum after cholesterol withdrawal (CWPS) or in vitro oxidized pig LDL (10 µg/ml) for 48 h. TUNEL staining was performed to assess apoptosis [7].

2.12. SMC proliferation and migration

To measure proliferation, SMC were seeded in 12-well plates in DMEM-10% FBS. Sub-confluent cells were starved for 96 h in DMEM-0.2% FBS. Thereafter, 0.2% FBS, 10% CPS, 10% HPS or 10% CWPS plus 0.5 μ Ci/ml of [3 H]thymidine were added simultaneously for 48 h. Cells were washed twice with PBS. Trichloroacetic acid-insoluble material was solubilized in 0.2 N NaOH and radioactivity was quantified in a β -scintillation liquid counter. To assess migration, scraping injury was performed on subconfluent cells in six-well plates [25]. Thereafter, 0.2% FBS, 10% FBS, 10% CPS, 10% HPS or 10% CWPS was added for 48 h. Cell nuclei were stained using the May-Grünwald-Giemsa method and the number of migrating cells and the migrating distance were assessed in ten high power fields (hpf) along the scraped line.

2.13. Extracellular matrix production

SMC were seeded in six-well plates in DMEM-10% FBS. Sub-confluent cells were maintained in 0.2% FBS, 0.2% CPS, 0.2% HPS or 0.2% CWPS for 9 days. Matrix production was assessed by supplementing medium with 5 μ Ci/well of [3 H]proline (Amersham) and quantifying incorporated [3 H]proline, as previously described [15].

2.14. Statistics

Groups were compared by non-parametric Kruskal–Wallis test or by non-parametric Mann–Whitney *U*-test. In vivo endothelial reactivity and ICUS data in diet pigs before and after cholesterol withdrawal were compared by Wilcoxon matched pairs paired test. Probability values of <0.05 were considered statistically significant.

3. Results

3.1. Plasma lipid levels and CRP

The cholesterol-rich diet induced a significant increase of total cholesterol, LDL-cholesterol, HDL-cholesterol and circulating ox-LDL but not of triglycerides within 4 weeks (Table 1). Thereafter, levels remained unchanged. After diet withdrawal, plasma lipids returned to baseline values within 4 weeks. Ox-LDL values 6 months after cholesterol withdrawal were similar to baseline values (Table 1). Levels of CRP were below detection limit in 13 out of 14 control pigs and in six out of seven pigs after cholesterol withdrawal, but above 3 mg/l in nine out of 12 hypercholesterolemic pigs (Table 1).

3.2. In vivo endothelial reactivity

Infusion of acetylcholine (10^{-4} M) induced vasoconstriction of the LAD in pigs on cholesterol-rich diet. In contrast, acetylcholine did not significantly change the lumen in control pigs or in pigs of the cholesterol withdrawal group after withdrawal of the cholesterol-rich diet. Endothelial independent vasodilatation was not different between groups, as shown in Table 1.

3.3. Coronary plaque load

In control pigs, intima was not detectable by ICUS. Cholesterol feeding induced significant coronary plaque progression (Fig. 1). Intimal areas in the proximal LAD measured by ICUS correlated with intimal areas determined by morphometric analysis of cross-sections ($R^2=0.64$, $P<0.05$) (Table 1). Cholesterol withdrawal did not result in a decrease of plaque load.

Table 1
Lipid values, endothelial function and atherosclerosis

	Control (1)	Hypercholesterolemic (2)	Cholesterol withdrawal (3)	ANOVA chi- square ^a <i>P</i>	1 vs. 2 <i>P</i>	1 vs. 3 <i>P</i>	2 vs. 3 <i>P</i>
Lipids and CRP	(<i>n</i> =14)	(<i>n</i> =12)	(<i>n</i> =7)				
LDL-C (mg/dl)	17 \pm 8	268 \pm 150	12 \pm 10	<0.001	<0.001	NS	<0.001
HDL-C (mg/dl)	29 \pm 9	81 \pm 19	27 \pm 5	<0.001	<0.001	NS	<0.001
TG (mg/dl)	65 \pm 36	49 \pm 27	99 \pm 46	NS	–	–	–
Ox-LDL (mg/dl)	0.73 \pm 0.15	2.67 \pm 1.29	0.85 \pm 0.11	<0.001	<0.001	NS	<0.001
CRP (mg/l)	<3 (12/14)	<3 (3/12)	<3 (6/7)	<0.01	<0.01	NS	<0.05
	4.7 (1/14)	5.4 \pm 2.6 (9/12)	3.8 (1/7)				
Endothelial function	(<i>n</i> =9)	(<i>n</i> =7)	(<i>n</i> =6)				
Acetylcholine ^a	–0.36 \pm 9.3%	–17.6 \pm 8.9%	–3.57 \pm 15.7%	0.019	<0.05	NS	<0.05
Nitroglycerine ^b	11.47 \pm 4.7%	7.29 \pm 2.7%	9.08 \pm 3.4%	NS	–	–	–
Lesion assessment	(<i>n</i> =14)	(<i>n</i> =12)	(<i>n</i> =7)				
Intimal area (mm ²)	0.15 \pm 0.11	0.88 \pm 0.70	1.18 \pm 0.45	<0.001	<0.001	<0.01	NS

Data are means \pm S.D. of *n* experiments per group.

^a Percentage diameter change after acetylcholine versus baseline.

^b Percentage diameter change after nitroglycerine versus baseline.

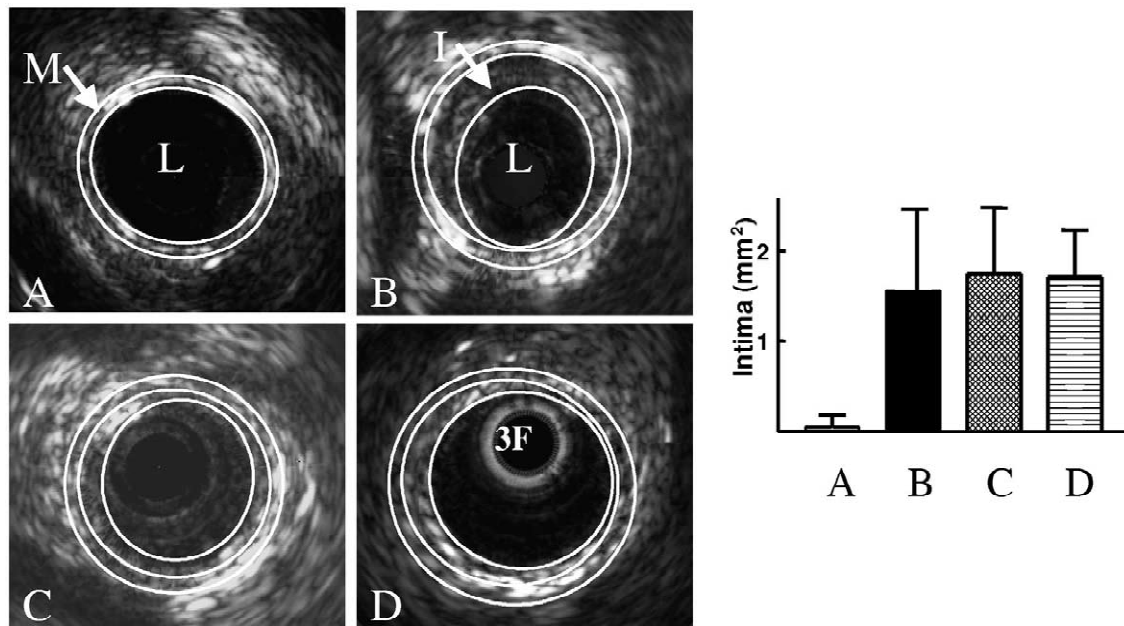


Fig. 1. Intra-coronary ultrasound of the proximal LAD from a control pig (A), a hypercholesterolemic pig (B), and a pig of the cholesterol withdrawal group before (C) and after cholesterol withdrawal (D). The atherogenic diet induced coronary atherosclerosis. Cholesterol withdrawal did not decrease plaque size. I, intima; L, lumen; M, media.

3.4. Coronary plaque type and composition

A total of five hypercholesterolemic pigs showed only early (Stary type I–III) lesions that mainly consisted of lipid-loaded macrophages (Fig. 2e), while seven hypercholesterolemic pigs had more advanced lesions (Stary IV–V). The cellular and extracellular composition of advanced lesions from the latter pigs was compared with those of size-matched lesions from pigs of the cholesterol withdrawal group, as illustrated in Figs. 2 and 3. Overall, advanced atherosclerotic lesions in the hypercholesterolemic group had a cell-rich cap area consisting of smooth muscle cells, a shoulder area containing macrophages and an acellular core. Lesions following cholesterol withdrawal did not show the cap/core structure. Smooth muscle cells were equally distributed throughout the lesions that were devoid of macrophages and lipids. Macrophage positive area, lipid stained area and ox-LDL stained area were, respectively, 20 ± 15 , 23 ± 17 , and $12 \pm 13\%$ in advanced atherosclerotic lesions and 4.8 ± 1.7 , 4.0 ± 2.6 and $2.2 \pm 1.6\%$ ($P < 0.05$ for all) in lesions following cholesterol withdrawal (Fig. 2). Myeloperoxidase stained area colocalized with macrophage positive area, as illustrated in Fig. 2d. Furthermore, lipid withdrawal resulted in increased collagen and extracellular matrix accumulation (Figs. 2i–p and 3).

3.5. SMC differentiation

Mean α -SM actin-positive plaque area was 1.5 times larger in the cholesterol withdrawal than in the hyper-

cholesterolemic group (29.3 ± 7.7 vs. $19.2 \pm 3.8\%$, $P < 0.05$). Smoothelin-positive plaque area was 2.8-fold higher in the cholesterol withdrawal than in the hypercholesterolemic group (19.0 ± 8.4 vs. $6.7 \pm 2.4\%$, $P < 0.01$). The percentage of the α -SM actin positive area that was positive for smoothelin was $64 \pm 21\%$ following cholesterol withdrawal compared to $35 \pm 11\%$ in hypercholesterolemic pigs ($P < 0.05$) (Figs. 2 and 3).

3.6. Extracellular matrix composition

Advanced atherosclerotic lesions in hypercholesterolemic pigs had a collagen-rich cap and a collagen-poor core. After cholesterol withdrawal, collagen density throughout the lesions was higher. Birefringence of the collagen in plaques was higher after cholesterol withdrawal, indicating more mature and organized triple helix collagen. The organized-to-total collagen ratio was significantly higher in the cholesterol withdrawal group than in the hypercholesterolemic group (Figs. 2 and 3). Plaque areas positive for type I collagen (9.7 ± 11 vs. $31 \pm 11\%$ of plaque area in hypercholesterolemic and cholesterol withdrawal group, respectively, $P < 0.001$) were similar to plaque areas positive for Sirius red under polarized light (8.6 ± 2.6 vs. $28 \pm 10\%$, respectively, $P < 0.001$). Elastin deposition, assessed by auto-fluorescence measurement and measurement of Verhoeffs-stained areas, was not significantly different between the hypercholesterolemic and cholesterol withdrawal group (Verhoeffs: 3.1 ± 1.8 vs. $4.1 \pm 2.5\%$, respectively, $P = \text{NS}$; autofluorescence: 6.4 ± 4.2 vs. $12 \pm 8.2\%$, respectively, $P = \text{NS}$).

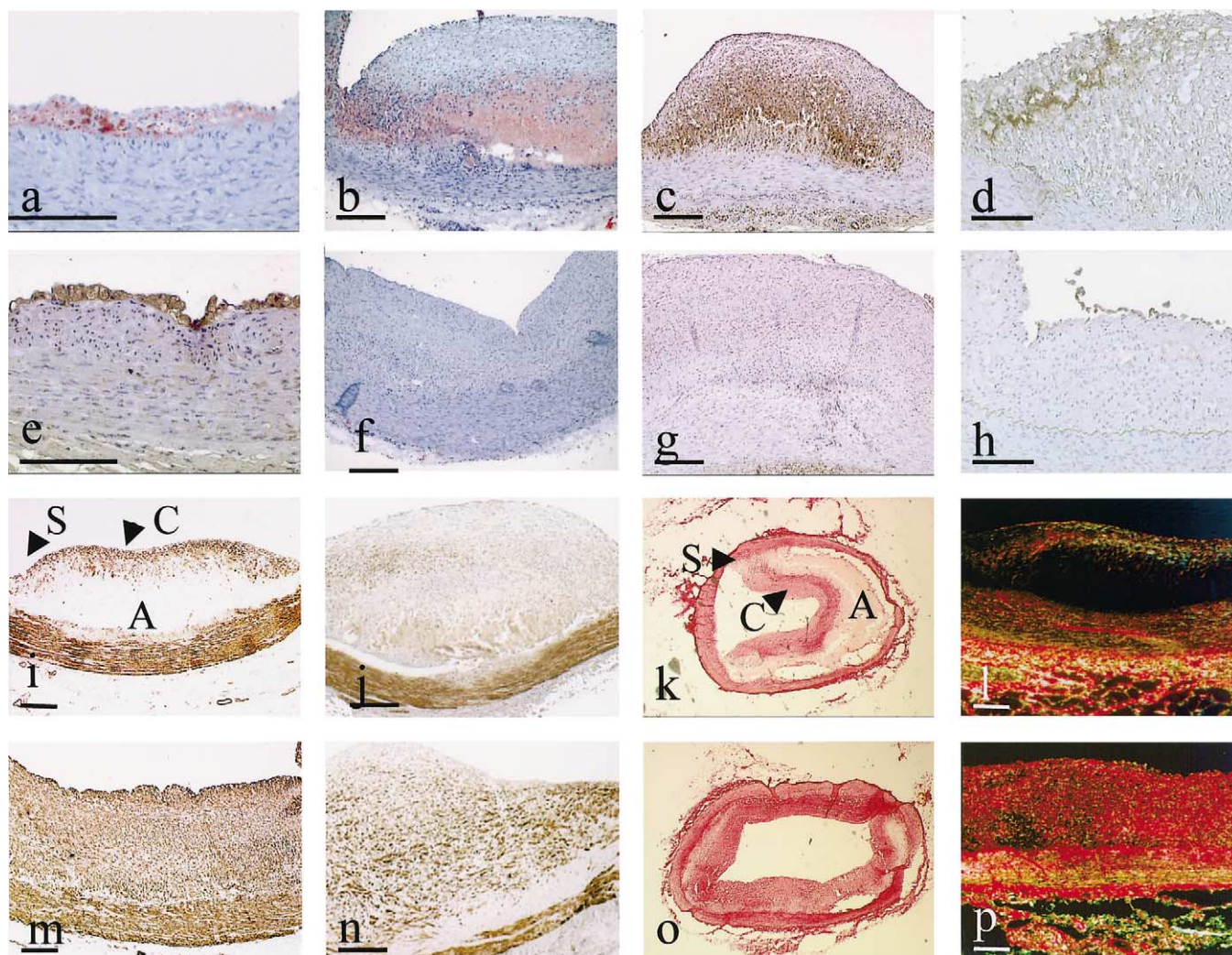


Fig. 2. Photomicrographs show an oil-red-O stained section of an early (a) and advanced atherosclerotic lesion (b) in the LAD from a hypercholesterolemic pig, and of a lesion in the LAD from a pig of the cholesterol withdrawal group (f). Macrophages were predominant in early (e) and advanced lesions (c) of hypercholesterolemic pigs. Macrophage-area colocalized with myeloperoxidase positive area (d, h). Dietary cholesterol withdrawal depleted the lesion of macrophages (g). α -SM actin and smoothelin staining revealed a higher number of more differentiated SMC in coronary plaques from pigs after cholesterol withdrawal (m, n) than from hypercholesterolemic pigs (i, j). Sirius red staining viewed under normal (k, o) and polarized light (l, p) showed the cap/core structure in advanced lesions of hypercholesterolemic pigs and the more homogeneous distribution of collagen after cholesterol withdrawal (100 μ m). Advanced lesions of the hypercholesterolemic pigs consist typically of a cap (C), shoulder (S) and a-cellular (A) core, whereas after cholesterol withdrawal lesions are more homogeneous of structure.

3.7. Apoptosis and proliferation

In advanced atherosclerotic lesions from hypercholesterolemic pigs, $1.7 \pm 0.72\%$ of all cells were TUNEL-positive, compared to $0.27 \pm 0.29\%$ of cells in lesions from pigs after cholesterol withdrawal (Fig. 4). TUNEL-positive cells colocalized with caspase-3 positive cells (Fig. 4) [26]. Combined TUNEL and PAS staining showed that $11 \pm 7.8\%$ of TUNEL-positive cells in advanced lesions were surrounded by a PAS-positive cage, indicating that they were of SMC-origin.

In advanced atherosclerotic lesions from hypercholesterolemic pigs, $3.4 \pm 3.1\%$ of cells were Ki67 positive

compared to $0.29 \pm 0.18\%$ of cells in lesions from pigs after cholesterol withdrawal. In hypercholesterolemic pigs, the lesion cap and shoulder region were particularly rich in proliferating cells, as illustrated in Fig. 4. Double staining for α -actin and Ki67 revealed less than 10% of all replicating cells to be SMC.

3.8. Effect of hypercholesterolemic serum on SMC apoptosis, migration, proliferation and matrix synthesis *in vitro*

HPS induced more apoptosis of SMC than FBS, CPS

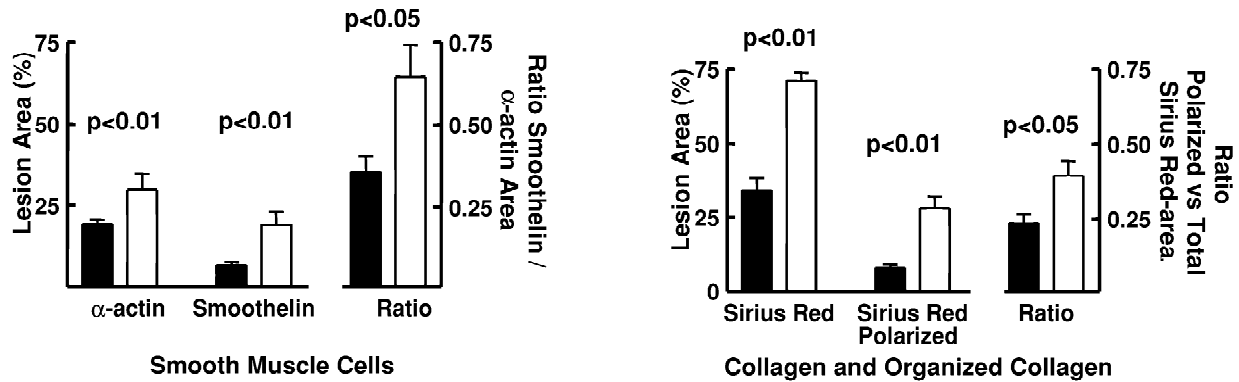


Fig. 3. Mean α -SM actin and smoothelin areas in advanced lesions from hypercholesterolemic pigs (■) and from pigs after dietary cholesterol withdrawal (□). Lesions from hypercholesterolemic pigs contained less smooth muscle cells that were less differentiated as indicated by the lower smoothelin-to- α -SM actin ratio. Lesions after cholesterol withdrawal contained more collagen that was more organized.

and CWPS (Fig. 5a). Apoptosis was also increased in the presence of 10 μ g/ml porcine in vitro oxidized LDL (17 ± 4.5 vs. $2.3 \pm 0.17\%$, $P < 0.05$, ox-LDL/0.2% FBS vs. 0.2% FBS). Compared to CPS and CWPS, HPS reduced the number of migrating SMC after scraping injury (Fig. 5b) as well as their migration distance (data not shown).

The proliferation rate, assessed by [3 H]thymidine incorporation, was not different when SMC were incubated with 10% FBS, 10% CPS, 10% HPS or 10% CWPS (Fig. 5c). Matrix synthesis in the presence of HPS was not

different from that in the presence of FBS, CPS or CWPS (Fig. 5d).

4. Discussion

Our study shows that cholesterol withdrawal decreased both plasma levels and plaque accumulation of ox-LDL and reduced inflammation as evidenced by a decrease of CRP. Dietary cholesterol withdrawal in miniature pigs

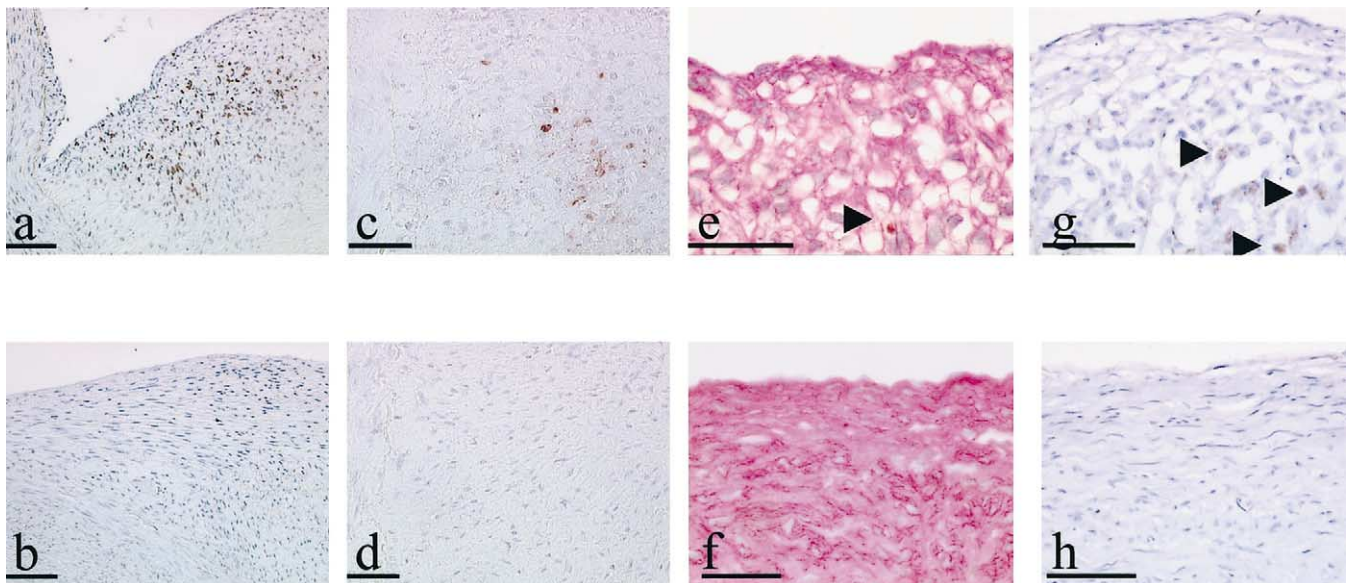


Fig. 4. Photomicrographs of Ki67 stained lesions from a hypercholesterolemic pig (a) and a pig after cholesterol withdrawal (b) show abundant cell proliferation in shoulder areas of atherosclerotic plaques in hypercholesterolemic pigs and reduced cell proliferation in lesions after cholesterol withdrawal. TUNEL staining demonstrated more TUNEL-positive cells in atherosclerotic lesions from hypercholesterolemic pigs (c) compared to lesions after cholesterol withdrawal (d). PAS staining shows more prominent extra-cellular matrix after cholesterol withdrawal (f) than in lesions of hypercholesterolemic pigs (e). Combining PAS and TUNEL staining showed TUNEL-positive cells surrounded by a matrix cage in atherosclerotic lesions (TUNEL-positive cell \blacktriangle). Caspase-3 stained lesions showed caspase-3 positive cells in a lesion from a hypercholesterolemic pig (g), but not in a lesion from a pig after cholesterol withdrawal (h; caspase-3 positive cell \blacktriangle) (50 μ m).

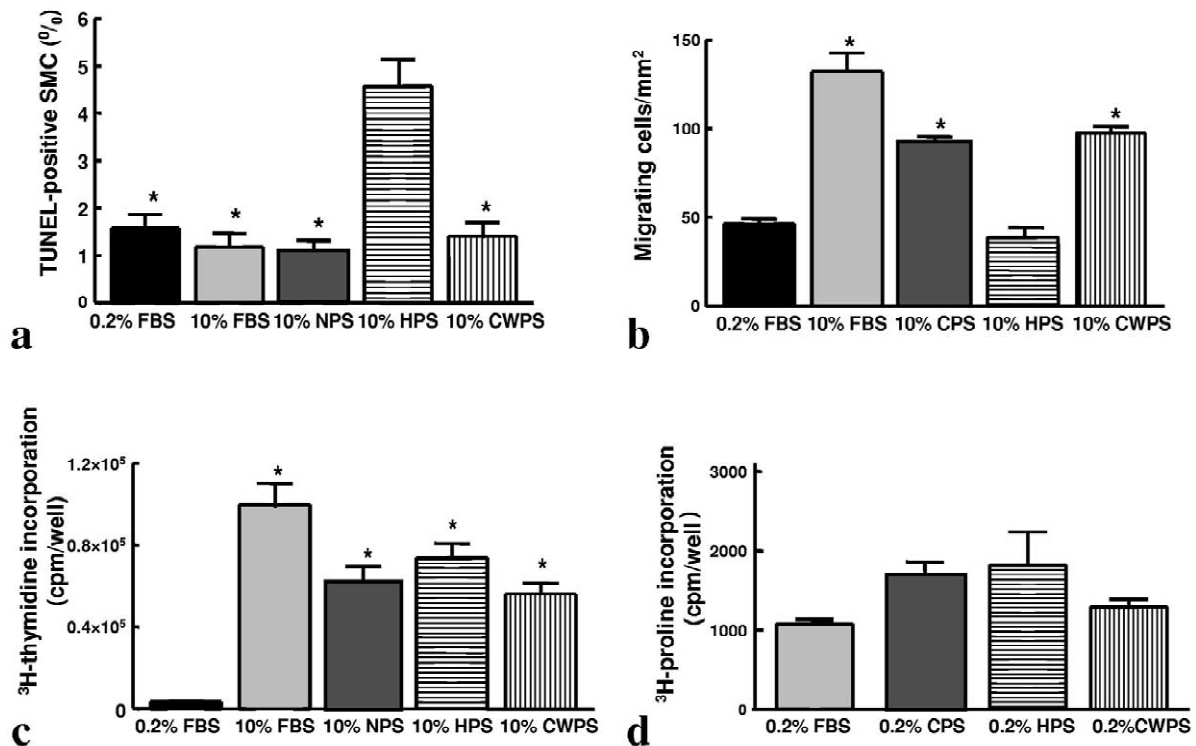


Fig. 5. Hypercholesterolemic serum induced more apoptosis of cultured coronary SMC than control serum or serum obtained after cholesterol withdrawal (a; ANOVA $P < 0.001$, $*P < 0.05$ vs. 10% HPS). HPS impaired migration of SMC compared to CPS, CWPS and FBS. There was no significant difference between control serum and serum obtained after cholesterol withdrawal (b; ANOVA $P < 0.0001$, $*P < 0.05$ vs. HPS). HPS had no effect on SMC proliferation compared to CWPS, CPS and FBS (c; ANOVA $P < 0.01$, $*P < 0.05$ vs. 0.2% FBS). HPS had no effect on extra-cellular matrix synthesis compared to CPS and CWPS (d; ANOVA $P = \text{NS}$).

induced a stable phenotype of coronary plaques without a regression of plaque size. Plaque stabilization was evidenced by decreased lipid and macrophage content, and accumulation of collagen and differentiated SMC in the former a-cellular core of these plaques. Our in vitro experiments support the hypothesis that the increase in SMC content of coronary plaques in the cholesterol withdrawal group is due to restored SMC migration and decreased SMC apoptosis. In vitro oxidized LDL mimicked the effect of hypercholesterolemic serum.

Smooth muscle cells are the only vascular cells that synthesize collagen fibers. Therefore, SMC number and function are important determinants of the mechanical strength of atherosclerotic plaques [27]. Cholesterol withdrawal induced accumulation of SMC in the former a-cellular core. A higher smoothelin-to- α -SM actin ratio evidenced a more differentiated SMC phenotype following cholesterol withdrawal. Differences in SMC content of lesions can be due to differences in proliferation, migration and/or apoptosis. Coronary plaques of both hypercholesterolemic pigs and pigs after cholesterol withdrawal contained few proliferating SMC, therefore migration rather than proliferation may determine SMC number. This is supported by our in vitro data showing that hypercholesterolemic serum impaired SMC migration but had no effect on SMC proliferation. Cholesterol withdrawal restored the

migratory properties on coronary SMC of porcine serum in vitro. We have previously shown that in vitro ox-LDL impaired migration of coronary SMC from hypercholesterolemic pigs [15]. Apoptosis of SMC may also determine SMC number. A PAS-positive cage suggesting SMC-origin surrounded ~10% of TUNEL-positive cells in plaques of hypercholesterolemic pigs. It is however difficult to exactly assess the origin of TUNEL-positive cells that surround the a-cellular core. Earlier studies have demonstrated that macrophages and ox-LDL induce SMC apoptosis [28] that can lead to cap thinning and mechanical weakening of the plaque [29]. Ox-LDL co-localized with apoptotic cells in human coronary lesions [30]. Plasma and plaque levels of ox-LDL were increased in hypercholesterolemic pigs. In vitro, hypercholesterolemic serum and ox-LDL induced SMC apoptosis. These data support the role of ox-LDL as an active component in hypercholesterolemic serum and coronary plaques for the induction of SMC apoptosis.

Cholesterol withdrawal increased both SMC and collagen content of coronary plaques. Extracellular matrix synthesis by SMC was not different in the presence of hypercholesterolemic serum compared to non-hypercholesterolemic serum. Hypercholesterolemia induces infiltration of macrophages in the intima that secrete proteolytic enzymes such as matrix metalloproteinases (MMP). They degrade the extracellular matrix and thereby contribute to

plaque remodeling and weakening [31–33]. We have previously shown that macrophage mediated degradation of extra-cellular matrix hampered the adhesion of SMC to the degraded matrix [15]. Cholesterol withdrawal restored endothelial function in coronary arteries that was associated with reduced macrophage infiltration in the coronary lesions. Increased collagen content of coronary plaques after cholesterol withdrawal is therefore most likely due to decreased macrophage mediated matrix degradation and increased SMC content, rather than to increased matrix synthesis by SMC. Furthermore, increased birefringence of collagen in plaques after cholesterol withdrawal indicates more mature and organized triple helix collagen [17].

Our data are in agreement with previous findings of Aikawa et al. [8,9] showing that lipid lowering was associated with increased expression of smooth muscle myosin heavy chain isoforms in the thoracic artery of rabbits and increased plaque collagen that was associated with reduced MMP activity.

Plaque stabilization was associated with reduced plasma levels of CRP and ox-LDL. Markers of inflammation may reflect plaque inflammation and seem promising in the risk prediction of cardiovascular disease [34,35]. In humans, circulating levels of ox-LDL are increased in patients with coronary artery disease [36] and are associated with increased levels of cell-adhesion molecules [37]. However, trials of the clinical usefulness of circulating ox-LDL to evaluate coronary risk are still lacking [38].

The LDL-hypercholesterolemia and the coronary atherosclerosis in miniature pigs are similar to human coronary artery atherosclerosis. In miniature pigs, like in humans, the atherosclerotic lesion formation in response to the atherogenic diet is variable but approximately half of them develop complex coronary plaques after a 9-month period of atherogenic diet. Differences in atherosclerosis susceptibility may depend on genetic determinants or interfering factors such as infection. These factors are not yet identified. We did not observe plaque rupture and coronary thrombosis in these miniature pigs. However, pigs on the atherogenic diet for 66 weeks were not studied. Further evolution of the plaques could therefore not be evaluated in this study. We cannot exclude that some of the changes in the cholesterol withdrawal group are related to the aging of the plaques or that a longer period of cholesterol-rich diet would result in plaque rupture or coronary thrombosis. Aging and SMC-senescence are indeed proposed to have an important role in plaque weakening and failure to maintain mechanical strength [39]. It may help explain why in these relatively young miniature pigs, we did not see plaque rupture in spite of the formation of complex calcified plaques. Acute coronary events are also less frequent in younger patients although serious plaque load can be present as demonstrated by ICUS [40].

In conclusion, we describe the characteristics of plaque stabilization by dietary cholesterol withdrawal in coronary arteries of miniature pigs. Cholesterol withdrawal reduced

inflammation and decreased macrophage and lipid content in coronary plaques. It increased collagen and SMC content and differentiation. Reduced inflammation and increase of the mechanical strength of the plaque may prevent rupture and coronary thrombosis in patients.

Acknowledgements

Peter Verhamme is a doctoral fellow of the Fonds voor Wetenschappelijk Onderzoek (FWO)-Vlaanderen. The Interuniversitaire Attractiepolen Program (P5/01/02) and FWO-grant G.0088.02 have supported this study.

References

- [1] Bucher HC, Griffith LE, Guyatt GH. Systematic review on the risk and benefit of different cholesterol-lowering interventions. *Arterioscler Thromb Vasc Biol* 1999;19:187–195.
- [2] Brown BG, Zhao XQ, Sacco DE et al. Lipid lowering and plaque regression. New insights into prevention of plaque disruption and clinical events in coronary disease. *Circulation* 1993;87:1781–1791.
- [3] Libby P. Current concepts of the pathogenesis of the acute coronary syndromes. *Circulation* 2001;104:365–372.
- [4] Ross R. Atherosclerosis—an inflammatory disease. *N Engl J Med* 1999;340:115–126.
- [5] Holvoet P, Theilmeyer G, Shivalkar B et al. LDL hypercholesterolemia is associated with accumulation of oxidized LDL, atherosclerotic plaque growth, and compensatory vessel enlargement in coronary arteries of miniature pigs. *Arterioscler Thromb Vasc Biol* 1998;18:415–422.
- [6] van der Loop FT, Gabbiani G, Kohnen G et al. Differentiation of smooth muscle cells in human blood vessels as defined by smoothelin, a novel marker for the contractile phenotype. *Arterioscler Thromb Vasc Biol* 1997;17:665–671.
- [7] Kockx MM, De Meyer GRY, Buyssens N et al. Cell composition, replication, and apoptosis in atherosclerotic plaques after 6 months of cholesterol withdrawal. *Circ Res* 1998;83:378–387.
- [8] Aikawa M, Rabkin E, Voglic SJ et al. Lipid lowering promotes accumulation of mature smooth muscle cells expressing smooth muscle myosin heavy chain isoforms in rabbit atheroma. *Circ Res* 1998;83:1015–1026.
- [9] Aikawa M, Rabkin E, Okada Y et al. Lipid lowering by diet reduces matrix metalloproteinase activity and increases collagen content of rabbit atheroma: a potential mechanism of lesion stabilization. *Circulation* 1998;97:2433–2444.
- [10] Small DM, Bond MG, Waugh D et al. Physicochemical and histological changes in the arterial wall of non-human primates during progression and regression of atherosclerosis. *J Clin Invest* 1984;73:1590–1605.
- [11] Armstrong ML, Megan MB. Lipid depletion in atheromatous coronary arteries in rhesus monkeys after regression diets. *Circ Res* 1972;30:675–680.
- [12] Maruffo CA, Portman OW. Nutritional control of coronary artery atherosclerosis in the squirrel monkey. *J Atheroscler Res* 1968;8:237–247.
- [13] Armstrong ML, Warner ED, Connor WE. Regression of coronary atheromatosis in rhesus monkeys. *Circ Res* 1970;27:59–67.
- [14] Holvoet P, Vanhaecke J, Janssens S et al. Oxidized LDL and malondialdehyde-modified LDL in patients with acute coronary syndromes and stable coronary artery disease. *Circulation* 1998;98:1487–1494.

- [15] Theilmeyer G, Quarck R, Verhamme P, Bochaton-Piallet M, Lox M. Hypercholesterolemia impairs vascular remodelling after porcine coronary angioplasty. *Cardiovasc Res* 2002;55:385–395.
- [16] Hasdai D, Best PJ, Cannan CR et al. Acute endothelin-receptor inhibition does not attenuate acetylcholine-induced coronary vasoconstriction in experimental hypercholesterolemia. *Arterioscler Thromb Vasc Biol* 1998;18:108–113.
- [17] Junqueira LC, Bignolas G, Brentani RR. Picrosirius staining plus polarization microscopy, a specific method for collagen detection in tissue sections. *Histochem J* 1979;11:447–455.
- [18] Blomfield J, Farrar JF. Fluorescence spectra of arterial elastin. *Biochem Biophys Res Commun* 1967;28:346–351.
- [19] Puchtler H, Waldrop FS. On the mechanism of Verhoeff's elastica stain: a convenient stain for myelin sheaths. *Histochemistry* 1979;62:233–247.
- [20] Stary HC, Chandler AB, Dinsmore RE et al. A definition of advanced types of atherosclerotic lesions and a histological classification of atherosclerosis. A report from the Committee on Vascular Lesions of the Council on Arteriosclerosis, American Heart Association. *Circulation* 1995;92:1355–1374.
- [21] Holvoet P, Theilmeyer G, Shivalkar B et al. LDL hypercholesterolemia is associated with accumulation of oxidized LDL, atherosclerotic plaque growth, and compensatory vessel enlargement in coronary arteries of miniature pigs. *Arterioscler Thromb Vasc Biol* 1998;18:415–422.
- [22] Christen T, Bochaton-Piallat ML, Neuville P et al. Cultured porcine coronary artery smooth muscle cells. A new model with advanced differentiation. *Circ Res* 1999;85:99–107.
- [23] Christen T, Verin V, Bochaton-Piallat M et al. Mechanisms of neointima formation and remodeling in the porcine coronary artery. *Circulation* 2001;103:882–888.
- [24] Ross R, Glomset JA. Atherosclerosis and the arterial smooth muscle cell: proliferation of smooth muscle is a key event in the genesis of the lesions of atherosclerosis. *Science* 1973;180:1332–1339.
- [25] Herren B, Garton KJ, Coats S et al. ADAM15 overexpression in NIH3T3 cells enhances cell–cell interactions. *Exp Cell Res* 2001;271:152–160.
- [26] Mallat Z, Ohan J, Leseche G et al. Colocalization of CPP-32 with apoptotic cells in human atherosclerotic plaques. *Circulation* 1997;96:424–428.
- [27] Shanahan CM, Weissberg PL. Smooth muscle cell phenotypes in atherosclerotic lesions. *Curr Opin Lipidol* 1999;10:507–513.
- [28] Libby P, Geng YJ, Aikawa M et al. Macrophages and atherosclerotic plaque stability. *Curr Opin Lipidol* 1996;7:330–335.
- [29] Kockx MM, Herman AG. Apoptosis in atherogenesis: implications for plaque destabilization. *Eur Heart J* 1998;19(Suppl G):G23–G28.
- [30] Okura Y, Brink M, Itabe H et al. Oxidized low-density lipoprotein is associated with apoptosis of vascular smooth muscle cells in human atherosclerotic plaques. *Circulation* 2000;102:2680–2686.
- [31] Henney AM, Wakeley PR, Davies MJ et al. Localization of stromelysin gene expression in atherosclerotic plaques by in situ hybridization. *Proc Natl Acad Sci USA* 1991;88:8154–8158.
- [32] Galis ZS, Sukhova GK, Lark MW et al. Increased expression of matrix metalloproteinases and matrix degrading activity in vulnerable regions of human atherosclerotic plaques. *J Clin Invest* 1994;94:2493–2503.
- [33] Brown DL, Hibbs MS, Kearney M et al. Identification of 92-kD gelatinase in human coronary atherosclerotic lesions. Association of active enzyme synthesis with unstable angina. *Circulation* 1995;91:2125–2131.
- [34] Ridker PM. Role of inflammatory biomarkers in prediction of coronary heart disease. *Lancet* 2001;358:946–948.
- [35] Ridker PM. High-sensitivity C-reactive protein: potential adjunct for global risk assessment in the primary prevention of cardiovascular disease. *Circulation* 2001;103:1813–1818.
- [36] Holvoet P, Mertens A, Verhamme P et al. Circulating oxidized LDL is a useful marker for identifying patients with coronary artery disease. *Arterioscler Thromb Vasc Biol* 2001;21:844–848.
- [37] Hulthe J, Fagerberg B. Circulating oxidized LDL is associated with increased levels of cell-adhesion molecules in clinically healthy 58-year old men (AIR study). *Med Sci Monit* 2002;8:CR148–CR152.
- [38] Tsimikas S, Witztum JL. Measuring circulating oxidized low-density lipoprotein to evaluate coronary risk. *Circulation* 2001;103:1930–1932.
- [39] Moon SK, Thompson LJ, Madamanchi N et al. Aging, oxidative responses, and proliferative capacity in cultured mouse aortic smooth muscle cells. *Am J Physiol Heart Circ Physiol* 2001;280:H2779–H2788.
- [40] De Franco AC, Nissen SE. Coronary intravascular ultrasound: implications for understanding the development and potential regression of atherosclerosis. *Am J Cardiol* 2001;88:7M–20M.